Acta Cryst. (1995). A51, 450–455

A Non-Uniform Reference Model for Maximum-Entropy Density Reconstructions from Diffraction Data

BY A. ZHELUDEV

CEA, Département de la Recherche Fondamentale sur la Matière Condensée/SPSMS/MDN, 17 rue des Martyrs, 38054 Grenoble CEDEX 9, France

R. J. PAPOULAR

Brookhaven National Laboratory, Upton, NY 11973, USA, and CEN Saclay, Laboratoire commun CEA-CNRS, 91191 Gif-sur-Yvette CEDEX, France

AND E. RESSOUCHE AND J. SCHWEIZER

CEA, Département de la Recherche Fondamentale sur la Matière Condensée/SPSMS/MDN, 17 rue des Martyrs, 38054 Grenoble CEDEX 9, France

(*Received* 25 *June* 1994; *accepted* 21 *September* 1994)

Abstract

Diffraction experiments provide information on the Fourier components of microscopic density distributions in crystals. To obtain the spatial densities themselves, an inverse Fourier problem has to be solved. The procedure is complicated by the presence of noise and incompleteness of the data. The application of the maximum-entropy (MaxEnt) principle was a breakthrough in density reconstruction, allowing high-quality density maps to be obtained without involving any *a priori* information concerning what the reconstructed density *should* look like. In this work, a procedure is proposed that incorporates *a priori* (*e.g.* theoretical) information into MaxEnt reconstructions of spin density distributions. It allows, on the one hand, the evaluation of the existing density models and, on the other, the precise investigation of what new information the experiment brings. Unlike traditional parameter-refinement techniques, the new method does not impose any strict constraints on the density to be reconstructed and is thus much more flexible. At the same time, it suppresses artifacts and yields high-quality density maps. The advantages of the new methods are illustrated by an example of spin density reconstruction based on real polarized neutron diffraction data.

Introduction

Diffraction experiments provide microscopic information on the scattering densities in crystals. In these methods, the Bragg intensities are measured, sometimes along with the phases of the related structure factors. The main information obtained is on structures: crystal structures from X-ray or neutron diffraction or magnetic structures from neutron diffraction. More and more experiments are performed to produce an accurate map of the scattering density itself: the charge density from X-ray experiments, the nuclear density from neutron experiments or the spin (magnetization) density from polarized neutron experiments.

In crystals, the scattering densities are periodic and the Bragg amplitudes are the Fourier components of these periodic distributions:

$$F(hkl) = \int \rho(\mathbf{r}) \exp(i\mathbf{kr})\, \mathbf{dr}. \qquad (1)$$

In principle, the scattering density $\rho(\mathbf{r})$ is given by the inverse Fourier transform of the experimental structure factors:

$$\rho(\mathbf{r}) = 1/V_0 \sum_{h,k,l} \exp(-i\,\mathbf{kr}) F(hkl), \qquad (2)$$

where the triple sum includes all the indices h, k, l, ranging from $-\infty$ to $+\infty$ and V_0 is the unit-cell volume. In fact, the number of measured reflections is limited and the inverse Fourier transformations that can be achieved are incomplete. Furthermore, the experimental structure factors are noisy, each $F(hkl)$ being measured with a standard deviation $\sigma(hkl)$. Therefore, the solution of the inverse problem is not unique. An infinite number of scattering density maps that are consistent with the measurements exist, namely all the maps for which the Fourier components corresponding to the measured Bragg reflections are compatible with the results of the measurements, with no condition at all on the Fourier components that have not been measured.

Among all the maps compatible with the data, the commonly adopted Fourier inversion procedure, which makes use of the series (2) with the sum limited to the structure factors actually measured, selects one of them: the map whose Fourier coefficients are equal to zero if

unmeasured and equal to their observed values otherwise. Obviously, this choice is completely arbitrary and does not consider the experimental uncertainties at all. Also, the unmeasured data are 'invented' and thus spatial correlations for which there is no experimental evidence are blindly imposed.

Several more motivated approaches to solving the inverse Fourier problem that arises in polarized neutron diffraction exist (see, for example, Gillon & Schweizer, 1989). Among these are the model refinement methods. They consist of constructing a parametrized model of the spin density and least-squares refining the parameters to best fit the experimental data. Another model-independent method recently appeared (Papoular & Gillon, 1990; Papoular & Delapalme, 1994). It uses the idea of maximum entropy (MaxEnt) (Gull & Skilling, 1984; Skilling & Gull, 1985) and its application was a breakthrough in polarized-neutron-data treatment.

The aim of this paper is to show that the previously mentioned data analysis, which is based on Bayesian (conditional) probabilities, with a 'flat' 'prior knowledge', may be improved by using an adapted model as 'prior knowledge'. An example of spin density reconstruction from a polarized neutron experiment is described in detail, in which the prior knowledge used is derived from theoretical chemistry principles.

Traditional MaxEnt for density reconstruction (uniform prior model)

The Bayesian approach to solving the inverse Fourier problem evaluates the probability for each of the possible reconstructed maps, given that the Fourier coefficients are the measured structure factors F_{obs} within the related experimental error bars. Such a conditional posterior probability can be written as $p(\text{map}|\text{data})$.

Here it is suitable to use the very general Bayes equality

$$p(A|B)p(B) = p(B|A)p(A), \tag{3}$$

which gives the posterior probability

$$p(\text{map}|\text{data}) = p(\text{data}|\text{map})p(\text{map})/p(\text{data}). \tag{4}$$

In this relation, $p(\text{data}|\text{map})$ is the likelihood. It represents the probability for the set of experimental data $F_{obs}(hkl)$ to be observed if the map *is* the real map. In other words, it represents the agreement between F_{obs} and F_{cal} and can be written as

$$p(\text{data}|\text{map}) \propto \exp(-\chi^2/2) \tag{5}$$

within a multiplicative factor. Here, $p(\text{map})$ is the prior probability. It represents all the knowledge pertaining to the density map that was available before the experiment that produced the set of data F_{obs} was performed. $p(\text{data})$, the intrinsic probability of the data, is a normalizing constant that we shall ignore in the remaining part of this paper. We are thus left with

$$p(\text{map}|\text{data}) \propto \exp(-\chi^2/2)p(\text{map}), \tag{6}$$

which means that the probability of a map, given the set of measured data $F_{obs}(hkl)$, is not expressed in terms of χ^2only, but also includes the prior probability of the map. The question of assigning the prior probability to a distribution arises.

In the traditional maximum-entropy method, the prior knowledge of the map is reduced to the assumption that all the points of the map are equally likely to carry the scattering density. Indeed, the crystallographic unit cell is divided into small pixels, inside which the scattering density is supposed to be constant: $\rho(\mathbf{r}) = \rho_i$. The *a priori* probability of finding some density in a given pixel is the same for each pixel (or 'flat'). In this case, it has been shown that the probability $p(\text{map})$ can be evaluated in combinatorial terms and expressed as the Boltzman entropy of the distribution:

$$\begin{aligned} p[\rho(\mathbf{r})] &= f(\text{Entropy}) \\ \text{Entropy}[\rho(\mathbf{r})] &= -\sum_i \tilde{\rho}_i \ln \tilde{\rho}_i, \end{aligned} \tag{7}$$

where f is a monotonous function and

$$\tilde{\rho}_i = \rho_i / \sum_j \rho_j \tag{8}$$

To select the map that provides the highest value of $p(\text{map}|\text{data})$, one has to optimize both the likelihood and the entropy of the distribution.

The method has been used for the reconstruction of charge densities from X-ray data (Sakata & Sato, 1990; Sakata, Mori, Kumazawa & Takata, 1990; Sakata, Uno, Takata & Mori, 1992) as well as for maps of nuclear densities from neutron data (Papoular, Prandl & Schiebel, 1991; Papoular & Schweizer, 1991; Papoular, Roth, Heger, Haluska & Kuzmany, 1993; Papoular, Ressouche, Schweizer & Zheludev, 1993; Sakata, Uno, Takata & Howard, 1993) or for spin densities from polarized neutron data (Papoular & Gillon, 1990; Papoular, Roth, Heger, Haluksa & Kuzmany, 1993; Papoular, Ressouche, Schweizer & Zheludev, 1993; Papoular & Delapalme, 1994; Boucherle *et al.*, 1992, 1993; Zheludev *et al.*, 1994*a*,*b*). In the two last cases, the extension of the method from strictly positive scattering densities to densities that can be either negative or positive has been achieved by considering a double distribution $\rho_i^+ = \rho^+(\mathbf{r}_i)$ and $\rho_i^- = \rho^-(\mathbf{r}_i)$ with $\rho(\mathbf{r}) = \rho^+(\mathbf{r}) - \rho^-(\mathbf{r})$ (Papoular & Gillon, 1992). The density maps obtained by this method, as compared to those resulting from the common inverse Fourier transformation, are tremendously improved. In particular, any substantial deviations from a background exhibited in the final map is really contained in the data, as it costs entropy compared to a map that would ignore such features.

Introduction of a non-uniform model as prior knowledge

In many cases, before the measurements are carried out, the experimentalist knows something about the investigated distribution such as, for example: the scattering density is due to electrons located mainly around the nuclei; the scattering density is due to p (or d or f) electrons; the scattering density is not too far from a theoretical model obtained from more or less elaborate calculations. In such cases, the flat prior knowledge used in traditional MaxEnt (FME), which considers all the different pixels as equally likely, is too weak a requirement in spite of its successes and has to be replaced. In general, the *a priori* knowledge of the scattering density is expressed as a spatial function $m(\mathbf{r})$, which can be used as a 'default model' of the required map. Skilling (1988) has shown that the prior knowledge can be encoded into the maximum-entropy formalism through the model $m(\mathbf{r})$ *via* a new definition of the entropy, which emerges from a rigorous Bayesian analysis:

$$\text{Entropy}[\rho(\mathbf{r})] = \sum_i [\rho_i - m_i - \rho_i \ln(\rho_i/m_i)]. \quad (9)$$

In the absence of any data, the global maximum of the entropy functional is reached for $\rho(\mathbf{r}) = m(\mathbf{r})$ and this equality would stand in the absence of data. In other words, one can say that any substantial departure from the model observed in the final map is really contained in the data as, with the new definition, it costs entropy.

These last considerations bring us to the fact that there are actually several ways of using MaxEnt with a default model (DMME) for density reconstructions:

(i) DMME allows one to obtain a better density map than the one resulting from the application of FME. Indeed, all the information missing in the experimental data but required to produce a reconstruction is not 'invented', but taken from *a priori* (*e.g.* theoretical) knowledge.

(ii) DMME provides a unique way to analyze a set of experimental data and to extract the pieces of physical or chemical information that are contained in it. The comparison of the final map with the default model shows exactly in what points of space the default model is unable to account for the experimental observations, that is, what *new* information the experiment brings.

(iii) In the case of competition between several models, the new method provides a way to use the experimental data to choose the best one. The models that give greater final values of entropy when used as defaults for DMME fit the data better.

A worked-out example

We demonstrate on a particular example how the use of a default model may improve the quality of MaxEnt reconstructions and help to interpret the experimental results. The new method was used to treat the polarized neutron diffraction data collected on a molecular compound, tetrabutylammonium tetracyanoethylenide $[Bu_4N]^+\{[TCNE]^{\bullet -}\}$ (Zheludev *et al.*, 1994*a*,*b*). The $[TCNE]^{\bullet -}$ molecule (Fig. 1) is a free radical and hence carries an unpaired electron, which is the cause for the paramagnetic behavior of the compound as a whole. According to elementary chemical considerations, the singly occupied molecular orbital (SOMO) of $[TCNE]^{\bullet -}$ is an antibonding MO, constructed of $|p_z\rangle$ (z axis is $\perp$ to this practically planar ion) atomic orbitals (AOs). The cation is a closed-shell system, thus no spin density is expected to reside on it. The aim of the experiment was to determine the spin density distribution in the anion, which is of fundamental importance for the understanding of the exchange interaction in several new molecular magnets (Miller, Epstein & Reif, 1988; Manriquez, Yee, McLean, Epstein & Miller, 1991).

$[TCNE]^{\bullet -}[Bu_4N]^+$ crystallizes in a monoclinic space group $P2_1/n$ ($a = 14.651$, $b = 8.446$, $c = 19.669$ Å, $\beta = 106.21°$). An aligned magnetization density was induced in the sample by applying an external magnetic field $H = 4.65$ T at $T = 1.6$ K. Altogether, 211 flipping ratios were collected up to $\sin\theta/\lambda = 0.36$ Å^{-1}. After the low-temperature structure was determined from a conventional neutron diffraction experiment, the corresponding magnetic structure factors $F_M(hkl)$ could be derived, together with the related error bars.

Historical perspective

For the reconstruction of the spin density from the F_M's, several methods have been used. The results obtained by direct Fourier inversion are shown in Fig. 2. First, the spin density in the asymmetric unit cell was reconstructed. A rectangular 'box' containing one $[TCNE]^{\bullet -}$ radical was then defined. The spin density confined in this box was projected along one of the box edges. It can be seen that the quality of this reconstruction is very low, the image is smeared out and the spin density is found all over the place, including far away from the nuclei.

The conventional (*i.e.* with a flat default model) MaxEnt 3D reconstruction is shown in Fig. 3. The historic MaxEnt algorithm was applied to reconstruct the density in the asymmetric cell on a $32 \times 32 \times 32$ pixel grid. A program based on the *MEMSYS*-3 subroutine library (Gull & Skilling, 1989) was used for this. The

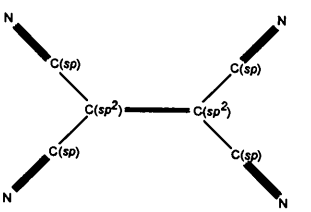

Fig. 1. Structural formula of the $[TCNE]^{\bullet -}$ radical ion.

projection procedure described above was then implemented to obtain this 2D image. The features of the spin density distribution are well discernible. In particular, the main part of the spin is found on the central sp^2 C atoms and the N atoms. It is notable that the spin density on the central C atoms is not centered but rather shifted outwards away from the C=C bond. This means that the antibonding bent character of the SOMO is strongly emphasized in this radical-ion. Is this feature indeed present in the experimental data or is it an artifact due to the reconstruction method?

This question was finally answered by modeling the spin density (Zheludev *et al.*, 1994*a*,*b*). The density was expanded into a multipolar series around the nuclei (Brown, Capiomont, Gillon & Schweizer, 1979) and the population coefficients were refined to best fit the experimental data. The problem that was encountered was that an accurate description of the deformation of the spin density on the C=C bond required too many multipolar functions from a standard basis set. As a result, too many parameters were used to model the density on a single atomic site and the model became overparametrized. It took a lot of trial refinements and intuition to eliminate the nuisance parameters and leave only those really vital for modeling the effect. The technique described in this paper shows a standard procedure which yields similar results, requires less labour and is much more justified in the sense of information theory.

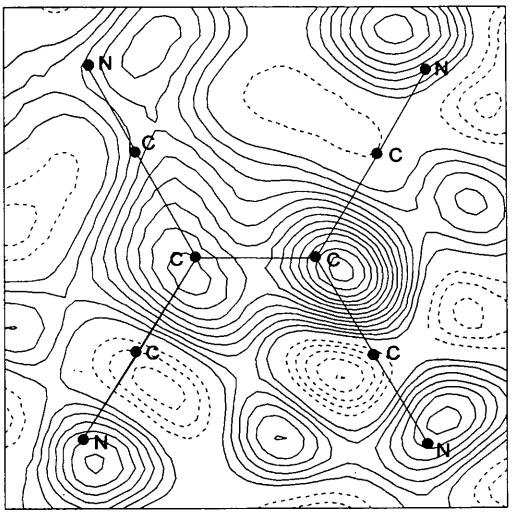

Fig. 2. Spin density in $[TCNE]^{\bullet-}[Bu_4N]^+$ obtained by Fourier inversion and subsequent projection onto the molecular plane of $[TCNE]^{\bullet-}$. Contours are $0.01\mu_B$ Å^{-2}. Negative contours are dashed.

Application of our new method: using a non-uniform prior model

First, a default model (DM) was constructed. The spin density was described in terms of individual atomic magnetic Slater-type orbitals ψ_i:

$$S(\mathbf{r}) = \sum_i S_i \psi_i(\mathbf{r}) \psi_i^*(\mathbf{r}). \qquad (10)$$

The S_i coefficients are the atomic spin populations. Elementary molecular orbital considerations suggest including $|2p_z\rangle$ orbitals for the N and sp^2 C sites. Note that the axial symmetry (absence of off-centering) of the spin density on the central C sites is intrinsic to this choice of DM. The values for the S_i were taken from local spin density (LSD) calculations (Zheludev *et al.*, 1994*a*,*b*). A projection of the theoretical spin density $S(\mathbf{r})$ onto the molecular plane of the radical is shown in Fig. 4.

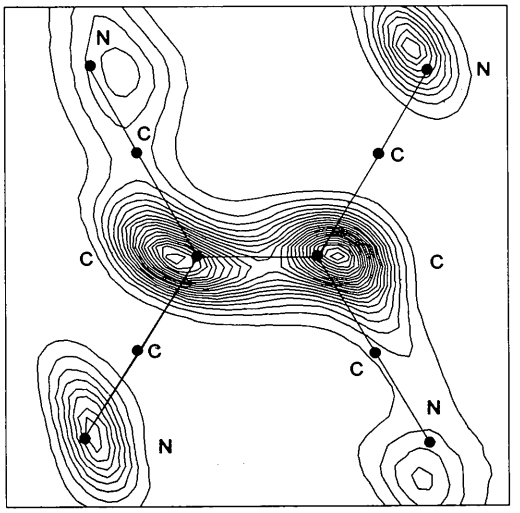

Fig. 3. Spin density $[TCNE]^{\bullet-}[Bu_4N]^+$ obtained by traditional flat-model MaxEnt reconstruction and subsequent projection onto the molecular plane of $[TCNE]^{\bullet-}$. Contours are $0.01\mu_B$ Å^{-2}.

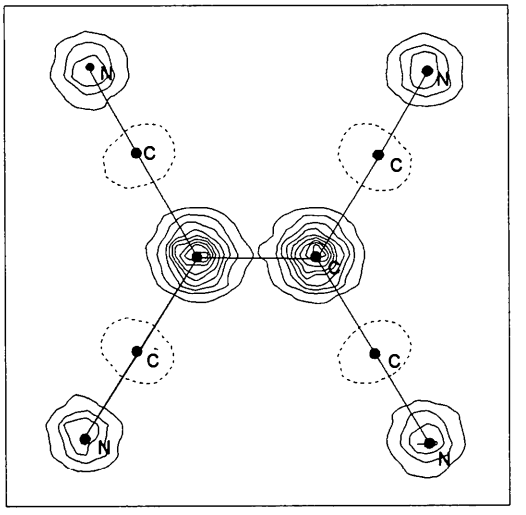

Fig. 4. Atomic orbital model for the spin density in $[TCNE]^{\bullet-}[Bu_4N]^+$ projected onto the molecular plane of $[TCNE]^{\bullet-}$. Contours are $0.05\mu_B$ Å^{-2}. Negative contours are dashed (step $0.01\mu_B$ Å^{-2}).

A non-trivial point is that this model density is negative in some points of space since the spin population of the four *sp* C atoms is negative. The model density in (9) plays the role of a Lebegian measure ('weight') assigned to the pixels and is thus essentially positive. One way to overcome this problem is to use two model densities, one for the positive part ρ_i^+ and one for the negative contribution ρ_i^-. In this work, we have used another approach adopted in the *MEMSYS*-3 subroutine package. The absolute value $\tilde{S}(\mathbf{r}) = |S(\mathbf{r})|$ of (10) was utilized for both ρ_i^+ and ρ_i^-. The algorithm was given full freedom to choose the sign of spin density in accord with the experimental data.

A 3D $32 \times 32 \times 32$ array of pixels representing the asymmetric unit cell was filled with values calculated using this DM $\tilde{S}(\mathbf{r})$. This simple atomic orbital DM was then used to reconstruct the spin density in the crystal using the historical MaxEnt algorithm. The result (in projection) is shown in Fig. 5. The map of differences between this reconstruction and the theoretical density $S(\mathbf{r})$ is presented in Fig. 6.

Discussion

Comparing Fig. 3 and Fig. 5, one readily sees that the new MaxEnt with a default atomic orbital model (DMME) gives reconstructions of much higher quality than the traditional FME. The information necessary to construct a spatial density, which is missing in the experimental data, is not invented, which it is when using Fourier inversion. Neither does the algorithm reconstruct it trying to avoid spatial correlations not present in the data, like FME. On the contrary, the missing information is taken from a theoretical model.

Fig. 6 demonstrates that, if the model is unable to fit the experimental data, the new information contained in the latter shows up in the reconstruction. The DMME reconstruction is not simply a reproduction of the DM. It points out exactly where the DM fails to describe the spin distribution. According to the latter, the spin density is centered on the sp^2 carbon sites. The DMME reconstruction shows that, in reality, a significant off-centering is present. The fact that the calculated shift of the spin density is symmetrical on the two sites proves the reliability of the result. Another feature contained in the data, but not in the model, is the inequality of the spin populations of the N atoms.

Unlike FME, DMME recovers the correct signs of the spin population of three of the four *sp* C atoms. Thus, DMME does more than simply use the information contained in the DM to fill in the gaps in the incomplete data. Indeed, it makes better use of the information that *is* contained in the latter.

It has to be emphasized that the DMME reconstruction, like FME and unlike model refinement (*e.g.* multipolar expansion) reconstructions, still fits the experimental data, $\chi^2 = 1$ exactly. In DMME, the DM affects only the entropy functional and not the likelihood itself (χ^2 term). It is a much 'softer' way of introducing *a priori* knowledge into the data treatment than parameter refinement methods, which very severely constrain the possible reconstructions. Any feature present in the data has the opportunity to manifest itself.

Naturally, some indirect 'pressure' on the reconstruction is still exerted by the model. The space in the crystal is not treated as homogeneous, as opposed to FME. For

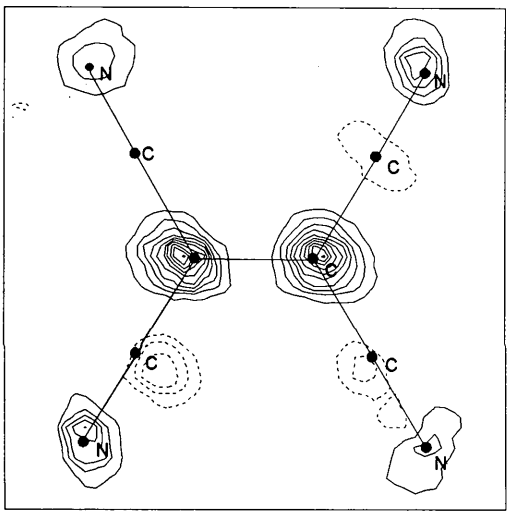

Fig. 5. Spin density in $[TCNE]^{\bullet-}[Bu_4N]^+$ obtained by MaxEnt reconstruction using the default model shown in Fig. 4 and subsequent projection onto the molecular plane of $[TCNE]^{\bullet-}$. Contours are $0.05\mu_B$ Å^{-2}. Negative contours are dashed (step $0.01\mu_B$ Å^{-2}).

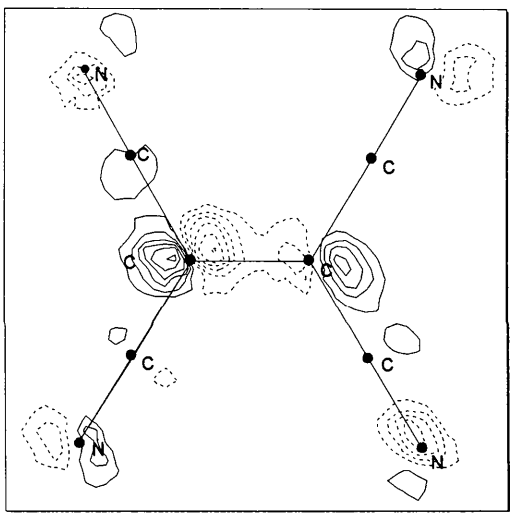

Fig. 6. Difference between the reconstructed (Fig. 5) and model (Fig. 4) spin densities in $[TCNE]^{\bullet-}[Bu_4N]^+$ projected onto the molecular plane of $[TCNE]^{\bullet-}$. Contours are $0.025\mu_B$ Å^{-2}. Negative contours are dashed.

example, the same deviation of the reconstructed density from the value of the DM in points of space where the DM is close to zero costs more entropy than in those points where the value of DM is large. In the case of spin densities, no serious problem is anticipated since there is no doubt that the spin density rapidly decays with distance from the nuclei. Rather, this effect is desirable since it favors localized densities and eliminates artifacts. On the contrary, close to the nuclei where the DM is large, a deviation from DM is less 'costly' and more freedom of the spin density shape is allowed.

If the existence of scattering density in regions of space where the DM approaches zero is plausible, the DM should be modified in such a way that this deviation from zero would not be so 'expensive' in terms of entropy. For example, $m(\mathbf{r})$ may be replaced by $m'(\mathbf{r}) = \max[m(\mathbf{r}), m_0]$, where m_0 is a positive constant.

Concluding remarks

The introduction of a non-uniform prior model of the scattering density greatly enhances the quality of MaxEnt density reconstructions and also provides a means to further improve our modeling by comparing the model (prior) density to the MaxEnt (posterior) density, which fits the data exactly.

Although the proposed procedure makes use of a model, it is not a parametrized process. It is still a direct method as the reconstructed density is not constrained by the model, which is used as a reference only for default.

References

BOUCHERLE, J.-X., HENRY, J.-Y., PAPOULAR, R., ROSSAT MIGNOD, J., SCHWEIZER, J. & TASSET, F. (1992). *J. Magn. Magn. Mater.* **104–107**, 630–632.

BOUCHERLE, J.-X., HENRY, J.-Y., PAPOULAR, R., ROSSAT MIGNOD, J., SCHWEIZER, J., TASSET, F. & UIMIN, G. (1993). *Physica (Utrecht)*, **B192**, 25–38.

BROWN, P. J., CAPIOMONT, A., GILLON, B. & SCHWEIZER, J. (1979). *J. Magn. Magn. Mater.* **14**, 289–294.

COLLINS, D. M. (1982). *Nature (London)*, **298**, 49–51.

GILLON, B. & SCHWEIZER, J. (1989). *Molecules in Physics, Chemistry and Biology*, Vol. II, edited by J. MARWANI, p. III. Dordrecht: Kluwer Academic Publishers.

GULL, S. F. & SKILLING, J. (1984). *IEE Proc.* **131**, 646–659.

GULL, S. F. & SKILLING, J. (1989). *MEMSYS User's Manual.* Maximum Entropy Data Consultants Ltd, 33 North End, Meldreth, Royston SG8 6NR, England.

MANRIQUEZ, J. M., YEE, G. T., MCLEAN, R. S., EPSTEIN, A. J. & MILLER, J. S. (1991). *Science*, **252**, 1415–1417.

MILLER, J. S., EPSTEIN, A. J. & REIFF, W. M. (1988). *Chem. Rev.* **88**, 201–220.

PAPOULAR, R. J. & DELAPALME, A. (1994). *Phys. Rev. Lett.* **72**, 1486–1489.

PAPOULAR, R. J. & GILLON, B. (1990). *Neutron Scattering Data Analysis*, edited by M. W. JOHNSON. *Inst. Phys. Conf. Ser.* No. 107, pp. 101–116.

PAPOULAR, R. J. & GILLON, B. (1992). *Europhys. Lett.* **13**, 429–434.

PAPOULAR, R. J., PRANDL, W. & SCHIEBEL, P. (1991). *Maximum Entropy and Bayesian Methods*, edited by G. ERICKSON, C. RAY-SMITH & P. NEUDORFER, pp. 359–376. Dordrecht: Kluwer Academic Publishers.

PAPOULAR, R. J., RESSOUCHE, E., SCHWEIZER, J. & ZHELUDEV, A. (1993). *Fundamental Theories in Physics*, Vol. 53, *Maximum Entropy and Bayesian Methods*, edited by A. MOHAMMAD-DJAFARI, and G. DEMOMENT, pp. 311–318. Dordrecht: Kluwer Academic Publishers.

PAPOULAR, R. J., ROTH, G., HEGER, G., HALUSKA, M. & KUZMANY, H. (1993). *Proceedings IWEP NM93*, edited by H. KUZMANY. *Springer Series in Solid State Sciences*, No. 117, pp. 189–194.

PAPOULAR, R. J. & SCHWEIZER, J. (1991). Procedings of the 6th International Neutron School on Neutron Physics, Alushta, Russia, 8–18 October 1991, pp. 170–189.

SAKATA, M., MORI, R., KUMAZAWA, S. & TAKATA, M. (1990). *J. Appl. Cryst.* **23**, 526–534.

SAKATA, M. & SATO, M. (1990). *Acta Cryst.* A**46**, 263–270.

SAKATA, M., UNO, T., TAKATA, M. & HOWARD, C. (1993). *J. Appl. Cryst.* 159–165.

SAKATA, M., UNO, T., TAKATA, M. & MORI, R. (1992). *Acta Cryst.* B**48**, 591–598.

SKILLING, J. (1988). *Maximum Entropy and Bayesian Methods in Science and Engineering*, Vol. 1, edited by G. J. ERICKSON & C. R. SMITH, pp. 173–187. Dordrecht: Kluwer Academic Publishers.

SKILLING, J. & GULL, S. F. (1985). *Maximum Entropy and Bayesian Methods in Inverse Problems*, edited by C. RAY-SMITH & W. T. GANDY JR, pp. 28–139. Dordrecht: Reidel.

ZHELUDEV, A., GRAND, A., RESSOUCHE, E., SCHWEIZER, J., MORIN, B., EPSTEIN, A. J., DIXON, D. & MILLER, J. S. (1994*a*). *Angew. Chem.* In the press.

ZHELUDEV, A., GRAND, A., RESSOUCHE, E., SCHWEIZER, J., MORIN, B., EPSTEIN, A. J., DIXON, D. & MILLER, J. S. (1994*b*). *J. Am. Chem. Soc.* In the press.